JOM 23945

Synthesis and interconversion of *triangulo* cluster compounds of platinum with isocyanide and phosphine ligands

Jane L. Haggitt [a] and D. Michael P. Mingos [b]

[a] *Inorganic Chemistry Laboratory, University of Oxford, South Parks Road, Oxford OX1 3QR (UK)*
[b] *Department of Chemistry, Imperial College of Science Technology and Medicine, South Kensington, London SW7 2AY (UK)*

(Received June 8, 1993)

Abstract

$Pt(COD)_2$ (COD = cyclo-octadiene) has proved to be a versatile starting compound for the synthesis of platinum *triangulo*-cluster compounds, many of which could not be synthesised by other routes. The reaction of $Pt(COD)_2$ with CNC_8H_9 and PCy_3 (Cy = cyclo-hexyl) resulted in the formation of cluster compounds that could not be obtained by substitution reactions based on related *triangulo* cluster compounds. The structure of $[Pt_3(\mu\text{-}CNC_8H_9)_3(PCy_3)_3]$ has been determined by a single crystal X-ray diffraction study, and sheds light on the steric interactions in this class of cluster compound. The interconversion reactions of the cluster compounds synthesised by this route have been studied.

1. Introduction

Mononuclear platinum(0) complexes are useful precursors for the synthesis of homonuclear cluster compounds of platinum. Compounds such as $[Pt_3(\mu\text{-}CN^tBu)_3(CN^tBu)_3]$, $[Pt_3(\mu\text{-}CO)_3(P^iPr_2Ph)_3]$, $[Pt_3(\mu\text{-}CO)_3(PMePh_2)_4]$, $[Pt_4(\mu\text{-}CO)_5(PEt_3)_4]$ and $[Pt_3(\mu\text{-}SO_2)_3(PCy_3)_3]$ have all been synthesised from either $Pt(COD)_2$ or its derivative, $Pt(C_2H_4)_2(PR_3)$ [1–5]. The nuclearity of platinum clusters containing carbonyl and phosphine ligands is sensitive to the steric and/or the electronic properties of the phosphine used. 42- and 44-electron trinuclear, 58-electron tetranuclear and 70-electron pentanuclear clusters have all been obtained in this manner. Platinum clusters containing only SO_2 and phosphine ligands, however, tend to be 42-electron trinuclear compounds, and no larger clusters containing only these ligands have been reported. In contrast, palladium tends to form 58-electron tetranuclear and 72-electron pentanuclear clusters such as $[Pd_4(SO_2)_3(PMe_3)_5]$ and $[Pd_5(SO_2)_4(PPh_3)_5]$ [6,7].

The substitution reactions of $[Pt_3(\mu\text{-}SO_2)_3(PCy_3)_3]$ and $[Pt_3(\mu\text{-}CO)_3(PCy_3)_3]$ with 2,6-dimethylphenylisocyanide (CNC_8H_9) have been studied by Mingos and co-workers [8,9]. It was found that with $[Pt_3(\mu\text{-}SO_2)_3(PCy_3)_3]$, addition of two equivalents of CNC_8H_9 gave $[Pt_3(\mu\text{-}SO_2)_2(CNC_8H_9)_2(PCy_3)_3]$. Addition of three equivalents resulted in cluster degradation to give the dimeric compound $[Pt_2(\mu\text{-}SO_2)(CNC_8H_9)_2(PCy_3)_2]$. In these reactions the isocyanide ligand remained in a terminal position. In contrast, the reaction of $[Pt_3(\mu\text{-}CO)_3(PCy_3)_3]$ with CNC_8H_9 resulted in substitution of the phosphine with no degradation of the cluster [9]. These reactions are illustrated in Fig. 1.

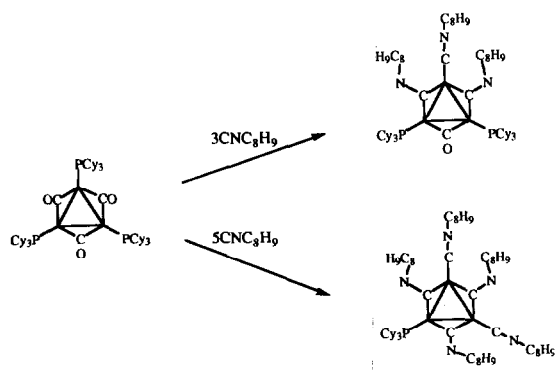

Fig. 1. Products resulting from the reaction of $[Pt_3(CO)_3(PCy_3)_3]$ and CNC_8H_9.

Correspondence to: Professor D.M.P. Mingos.

* Dedicated to Professor Michael Lappert in recognition of his outstanding contributions to organometallic chemistry.

0022-328X/93/$6.00

With three equivalents of CNC_8H_9, $[Pt_3(\mu\text{-}CO)(\mu\text{-}CNC_8H_9)_2(CNC_8H_9)(PCy_3)_2]$ was formed and with five equivalents, $[Pt_3(\mu\text{-}CNC_8H_9)_3(CNC_8H_9)_2(PCy_3)]$ was formed.

The structures of these cluster compounds showed that the bridging isocyanide ligands were severely bent at the nitrogen atoms, making it sterically unfavourable for them to bridge between two $Pt(PCy_3)$ units. The substitution of a bridging CO ligand by CNC_8H_9 was thought to labilise an adjacent terminal phosphine by virtue of these steric interactions, leading to substitution by another isocyanide molecule. It was argued that the two products were formed in preference to the more symmetrically substituted derivative owing to the steric requirements of the bridging isocyanides.

The fully substituted cluster, $[Pt_3(\mu\text{-}CNC_8H_9)_3(CNC_8H_9)_3]$ could not be synthesised by this method, but has been obtained from the reaction of $Pt(COD)_2$ with CNC_8H_9 [10]. It was therefore of interest to investigate whether the symmetrically-substituted cluster compound, $[Pt_3(\mu\text{-}CNC_8H_9)_3(PCy_3)_3]$, could be synthesised from a mononuclear complex such as $Pt(COD)_2$. The reaction of $Pt(COD)_2$ with a tertiary phosphine and CNC_8H_9 was therefore carried out in an attempt to produce such a cluster.

2. Results and discussion

2.1. Synthesis and characterisation of $[Pt_3(\mu\text{-}CNC_8H_9)_3(PCy_3)_3]$

When a solution of CNC_8H_9 in benzene was added to one of $Pt(COD)_2$ and PCy_3 in the same solvent in a 1:1:1 molar ratio a colour change from pale yellow to dark red was observed. After removal of the solvent under reduced pressure the product was recrystallised from CH_2Cl_2/MeOH to give red crystals. The product was formulated as $[Pt_3(\mu\text{-}CNC_8H_9)_3(PCy_3)_3]$ on the basis of microanalyses, IR and $^{31}P\{^1H\}$ NMR spectroscopy. The $^{31}P\{^1H\}$ NMR spectrum showed a complex multiplet centred at 53.1 ppm characteristic of a symmetrical 42-electron trinuclear platinum cluster with $^1J(P\text{–}Pt) = 4693$ Hz, $^2J(P\text{–}Pt) = 418$ Hz and $^3J(P\text{–}P) = 52$ Hz. $^{31}P\{^1H\}$ NMR spectra of $[Pt_3(\mu\text{-}X)_3(PR_3)_3]$ cluster compounds have been reported in detail by several workers [2,11,14]. The spectrum can be satisfactorily simulated as a superposition of the spectra derived from the spin systems of the four isotopomers:

A_3	(no ^{195}Pt nuclei, 29.6% abundance)
$A_2A'X$	(1 ^{195}Pt nuclei, 44.4% abundance)
$AA'A''XX'$	(2 ^{195}Pt nuclei, 22.2% abundance)
$AA'A''XX'X''$	(3 ^{195}Pt nuclei, 3.7% abundance)

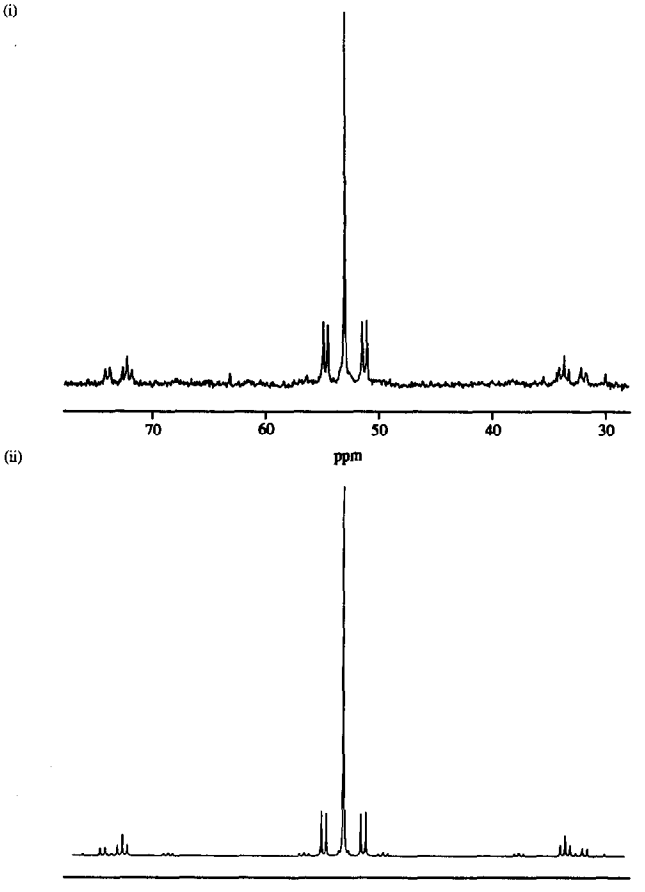

Fig. 2. $^{31}P\{^1H\}$ NMR spectrum of $[Pt_3(\mu\text{-}CNC_8H_9)_3(PCy_3)_3]$: (i) observed; (ii) simulated.

The single resonance due to the A_3 isotopomer defines the chemical shift. The fine structure from the most abundant complex, the $A_2A'X$ isotopomer, defines the nuclearity of the symmetrical cluster. The $^{31}P\{^1H\}$ NMR and the computer simulated spectra of $[Pt_3(\mu\text{-}CNC_8H_9)_3(PCy_3)_3]$ are shown in Fig. 2.

The IR spectrum as a Nujol mull showed four bands at 1836, 1760, 1696 and 1584 cm^{-1}, indicating the presence of bridging isocyanide ligands. There was no evidence for terminal isocyanide ligands. The presence of four bands in the cyanide bridging region suggests that the symmetry of the molecule in the crystalline state is significantly lower than the idealised D_{3h} symmetry.

Given that the cluster $[Pt_3(\mu\text{-}CNC_8H_9)_3(PCy_3)_3]$ could not be obtained by substitution reaction of $[Pt_3(\mu\text{-}CO)_3(PCy_3)_3]$ and that this was attributed to steric factors, it was of interest to see how the steric interactions between the ligands [12] are resolved in this cluster. An X-ray diffraction study of the compound was therefore undertaken and these results are discussed in Section 2.2.

TABLE 1. IR data for $[Pt_3(\mu\text{-}CNC_8H_9)_3(PR_3)_3]$

Cluster	Cone angle (°)	ν(CN) (cm^{-1})
$[Pt_3(\mu\text{-}CNC_8H_9)_3(PCy_3)_3]$	170	1836w, 1760m, 1696vs, 1584s
$[Pt_3(\mu\text{-}CNC_8H_9)_3(PBz_3)_3]$	165	1781m, 1702vs, 1600m, 1585s
$[Pt_3(\mu\text{-}CNC_8H_9)_3(PPh_3)_3]$	145	1878w, 1770sh, 1693vs, 1584s
$[Pt_3(\mu\text{-}CNC_8H_9)_3(PMe_3)_3]$	118	1675vs, 1585s

The analogous reaction between $Pt(COD)_2$, PR_3 and CNC_8H_9 was also successfully carried out with the phosphines PPh_3, PBz_3, PMe_2Ph and PMe_3 to give the clusters $[Pt_3(\mu\text{-}CNC_8H_9)_3(PR_3)_3]$. $[Pt_3(\mu\text{-}CNC_8H_9)_3(PPh_3)_3]$ and $[Pt_3(\mu\text{-}CNC_8H_9)_3(PBz_3)_3]$ were isolated as red crystalline compounds. $[Pt_3(\mu\text{-}CNC_8H_9)_3(PMe_3)_3]$ was obtained in quantitative yield but was isolated only as an oil. The compounds were characterised by $^{31}P\{^1H\}$ NMR and IR spectroscopy. $[Pt_3(\mu\text{-}CNC_8H_9)_3(PMe_2Ph)_3]$ was also obtained as an oil but could not be purified, and so was characterised using $^{31}P\{^1H\}$ NMR spectroscopy only. Details of the IR spectral data and $^{31}P\{^1H\}$ NMR data are given in Tables 1 and 2, respectively.

The ^1J(Pt–P) coupling constants for $[Pt_3(\mu\text{-}CNC_8H_9)_3(PR_3)_3]$ are about 400–900 Hz larger than those for the analogous $[Pt_3(\mu\text{-}SO_2)_3(PR_3)_3]$ clusters. The ^1J(Pt–P) coupling constant has been related to the s character of the Pt–P bond [13], which is affected by the electronic properties of the bridging ligand. It is possible that the weaker σ-donor and better π-acceptor properties of SO_2 relative to those of CNC_8H_9 reduces the s character of the Pt–P bond. A similar relationship [14] has been observed between $[Pt_3(\mu\text{-}CO)_3(PR_3)_3]$ and $[Pt_3(\mu\text{-}SO_2)_3(PR_3)_3]$.

2.2. X-Ray structural analysis of $[Pt_3(\mu\text{-}CNC_8H_9)_3(PCy_3)_3]$

Red crystals of $[Pt_3(\mu\text{-}CNC_8H_9)_3(PCy_3)_3]$ suitable for a single crystal X-ray analysis were obtained by the slow diffusion of MeOH into a toluene solution of the compound. Details of the data collection and refinement are summarised in Table 3. Selected bond lengths and angles are given in Table 4 and atomic coordinates are given in Table 5. The structure is illustrated in Figs. 3 and 4.

TABLE 3. Crystal data for $Pt_3(\mu\text{-}CNC_8H_9)_3(PCy_3)_3$

Formula	$C_{81}H_{126}N_3P_3Pt_3$
Formula weight	1820.098
Crystal system	Triclinic
Space group	$P\bar{1}$
a (Å)	15.022(3)
b (Å)	21.011(5)
c (Å)	14.957(8)
α (°)	93.14(3)
β (°)	119.83(3)
γ (°)	101.92(2)
V (Å)	3937.623
Z	2
D_c (g cm^{-3})	1.559
$F(000)$	1824
Linear absorption coefficient (cm^{-1})	55.577
Data collection	
X-radiation	Mo-Kα ($\lambda = 0.71069$ Å)
θ_{min}, θ_{max} (°)	1.50, 22.00
Min., max, h, k, l	−15, 15; −22, 22; −1, 15
ω-Scan width (°)	$0.95 + 0.35 \tan\theta$
Total data collected	10523
Total unique data	9534
Total observed data [$I > 3\sigma(I)$]	6963
Merging R factor	2.37%
Absorption correction	
Type	Azimuthal Scan profile
Min/max correction in θ	1.79, 2.38
Refinement	
No. of parameters	391
Ratio data : parameters	17.8
Weighting scheme (+ parameters)	Chebychev
	9.50, −4.53, 6.76
R	0.0450
R_w	0.0533

The three platinum atoms form an approximately equilateral triangle with Pt–Pt distances of 2.6859(6), 2.6848(5), and 2.6858(6) Å. These bond lengths fall within the range established for bridged Pt–Pt bonds, examples of which are given in Table 6.

The Pt–Pt bonds are shorter than those in $[Pt_3(\mu\text{-}SO_2)_3(PCy_3)_3]$ owing to the fact that the distances in these clusters depend in part on the size of the bridging atoms.

The conformations of the phosphine ligands are very similar, as are those of the isocyanide ligands, giving the molecule a pseudo three-fold rotation axis.

TABLE 2. $^{31}P\{^1H\}$ NMR data for $[Pt_3(\mu\text{-}CNC_8H_9)_3(PR_3)_3]$

Cluster	δ (ppm)	^1J(Pt–P) (Hz)	^2J(Pt–P) (Hz)	^3J(P–P) (Hz)
$[Pt_3(\mu\text{-}CNC_8H_9)_3(PCy_3)_3]$	53.1	4693	418	52
$[Pt_3(\mu\text{-}CNC_8H_9)_3(PBz_3)_3]$	40.4	4650	464	71
$[Pt_3(\mu\text{-}CNC_8H_9)_3(PPh_3)_3]$	47.7	4936	474	58
$[Pt_3(\mu\text{-}CNC_8H_9)_3(PMe_2Ph)_3]$	25.7	4457	463	68
$[Pt_3(\mu\text{-}CNC_8H_9)_3(PMe_3)_3]$	17.8	4316	443	70

TABLE 4. Selected bond lengths (Å) and bond angles (°) for $Pt_3(CNC_8H_9)_3(PCy_3)_3$

Pt(1)–Pt(2)	2.6859(6)	Pt(3)–P(3)	2.289(3)
Pt(1)–Pt(3)	2.6848(5)	Pt(3)–C(5)	2.06(1)
Pt(1)–P(1)	2.288(3)	Pt(3)–C(6)	2.09(1)
Pt(1)–C(4)	2.04(1)	N(4)–C(4)	1.24(1)
Pt(1)–C(6)	2.09(1)	N(4)–C(41)	1.41(2)
Pt(2)–Pt(3)	2.6858(6)	N(5)–C(5)	1.22(1)
Pt(2)–P(2)	2.290(3)	N(5)–C(51)	1.40(1)
Pt(2)–C(4)	2.04(1)	N(6)–C(6)	1.17(1)
Pt(2)–C(5)	2.05(1)	N(6)–C(61)	1.43(2)
Pt(3)–Pt(1)–Pt(2)	60.01(1)	P(3)–Pt(3)–Pt(1)	145.32(7)
P(1)–Pt(1)–Pt(2)	145.56(7)	P(3)–Pt(3)–Pt(2)	151.59(7)
P(1)–Pt(1)–Pt(3)	151.16(7)	C(5)–Pt(3)–Pt(1)	107.1(3)
C(4)–Pt(1)–Pt(2)	48.8(3)	C(5)–Pt(3)–Pt(2)	49.0(3)
C(4)–Pt(1)–Pt(3)	107.1(3)	C(5)–Pt(3)–P(3)	107.5(3)
C(4)–Pt(1)–P(1)	101.4(3)	C(6)–Pt(3)–Pt(1)	50.0(3)
C(6)–Pt(1)–Pt(2)	107.7(3)	C(6)–Pt(3)–Pt(2)	107.8(3)
C(6)–Pt(1)–Pt(3)	49.9(3)	C(6)–Pt(3)–P(3	100.4(3)
C(6)–Pt(1)–P(1)	106.7(3)	C(6)–Pt(3)–C(5)	143.4(4)
C(6)–Pt(1)–C(4)	143.6(4)	C(41)–N(4)–C(4)	141.1(10)
Pt(3)–Pt(2)–Pt(1)	59.97(1)	Pt(2)–C(4)–Pt(1)	82.2(4)
P(2)–Pt(2)–Pt(1)	151.51(7)	N(4)–C(4)–Pt(1)	131.6(8)
P(2)–Pt(2)–Pt(3)	145.16(7)	N(4)–C(4)–Pt(2)	139.2(9)
C(4)–Pt(2)–Pt(1)	48.9(3)	C(51)–N(5)–C(5)	141.0(10)
C(4)–Pt(2)–Pt(3)	107.1(3)	Pt(3)–C(5)–Pt(2)	81.6(4)
C(4)–Pt(2)–P(2)	107.6(3)	N(5)–C(5)–Pt(2)	132.7(9)
C(5)–Pt(2)–Pt(1)	107.5(3)	N(5)–C(5)–Pt(3)	140.4(9)
C(5)–Pt(2)–Pt(3)	49.4(3)	C(61)–N(6)–C(6)	140.2(11)
C(5)–Pt(2)–P(2)	100.7(3)	Pt(3)–C(6)–Pt(1)	80.1(4)
C(5)–Pt(2)–C(4)	144.2(4)	N(6)–C(6)–Pt(1)	142.0(9)
Pt(2)–Pt(3)–Pt(1)	60.01(1)	N(6)–C(6)–Pt(3)	132.8(9)

The phosphines are arranged in an eclipsed fashion with two cyclohexyl groups positioned above the metal plane and one below. The Pt–P distances are comparable with those found in other platinum clusters, although in this case the Pt–P bonds are not coplanar but deviate from the metal plane by an average of 10.4°. In the majority of these types of clusters the phosphorus atoms tend to lie in the same plane as the metal atoms.

The bridging carbon atoms lie below the Pt plane such that the dihedral angle between the metal plane and the Pt–C–Pt plane is, on average, 18.1°. Again this is relatively unusual, since the bridging atoms are normally coplanar with the metal atoms. Similar behaviour, however, is seen in $[Pt_3(\mu\text{-}CO)_3(P^tBu_2Ph)_3]$ [17], in which the CO ligands lie above the plane defined by the Pt atoms with an average dihedral angle of 7°. This was attributed to the steric demands of the P^tBu_2Ph ligands.

The isocyanide ligands are bent, with an average C–N–C angle of 140°, and are orientated so that the phenyl rings deviate from the perpendicular by 34.7°. The C–N–C angle is quite large compared to those in $[Pt_3(\mu\text{-}CN^tBu)_3(CN^tBu)_3]$ [1], $[Pt_3(\mu\text{-}CO)(\mu\text{-}CNC_8H_9)_2(CNC_8H_9)(PCy_3)_2]$ and $[Pt_3(\mu\text{-}CNC_8H_9)_3(CNC_8H_9)_2(PCy_3)]$, in which the angles are 132.7°, 128.5° and 132.0°, respectively.

In $[Pt_3(\mu\text{-}CO)(\mu\text{-}CNC_8H_9)_2(CNC_8H_9)(PCy_3)_2]$ and $[Pt_3(\mu\text{-}CNC_8H_9)_3(CNC_8H_9)_2(PCy_3)]$ the isocyanide ligands are coplanar with the metal plane and the phenyl rings are perpendicular to the metal plane. The terminal isocyanides, which occupy far less space than the phosphine ligands, allow the bridging isocyanides to bend more. In $[Pt_3(\mu\text{-}CNC_8H_9)_3(PCy_3)_3]$, the metal-bound ligand atoms all deviate from the metal plane owing to the steric requirements of the bridging isocyanide ligands and the phosphine ligands.

This is the first example of a platinum cluster in which an isocyanide ligand bridges between two $Pt(PCy_3)$ units. The cluster compound $[Pt_3Au(\mu\text{-}SO_2)_2(\mu\text{-}CNC_8H_9)(PCy_3)_4]PF_6$, which was characterised by FAB-MS, analytical and spectroscopic data [18], is also thought to contain a similar bridging isocyanide, although in this case the isocyanide is linear. An X-ray diffraction study of this compound was not undertaken however.

2.3. Synthesis of $[Pt_3(\mu\text{-}CNC_8H_9)_3(CNC_8H_9)(PCy_3)_2]$

By varying the stoichiometry used in the reaction between $Pt(COD)_2$, PCy_3 and CNC_8H_9 it proved possible to isolate the related cluster, $[Pt_3(\mu\text{-}CNC_8H_9)_3(CNC_8H_9)(PCy_3)_2]$. This compound has not previously been reported since it cannot be made via the substitution reaction of $[Pt_3(\mu\text{-}CO)_3(PCy_3)_3]$ with CNC_8H_9.

When a solution of CNC_8H_9 in benzene was added to one of $Pt(COD)_2$ and PCy_3 in benzene in the ratio 4:3:2 a colour change to dark red was observed. After 1 h stirring the solvent was removed under reduced pressure and the product recrystallised from CH_2Cl_2/EtOH to give orange crystals of $[Pt_3(\mu\text{-}CNC_8H_9)_3(CNC_8H_9)(PCy_3)_2]$. The cluster was characterised by analysis and $^{31}P\{^1H\}$ NMR and IR spectroscopy. The IR spectrum showed four bands at 2109 cm^{-1} (corresponding to the terminal isocyanide), and 1890, 1697 and 1586 cm^{-1} (indicating the presence of bridging isocyanides). The $^{31}P\{^1H\}$ NMR spectrum showed a complex multiplet centred at 63.3 ppm, consistent with the structure shown in Fig. 5. Details of the coupling constants are given in Table 7. A satisfactory computer simulation was achieved on the basis of the six isotopomers.

A_2	(no ^{195}Pt nuclei, 29.6% abundance)
A_2Y	(1 ^{195}Pt nucleus, Y, 14.8% abundance)
AA'X	(1 ^{195}Pt nucleus, X, 29.6% abundance)
AA'XY	(2 ^{195}Pt nuclei, X, Y, 14.8% abundance)
AA'XX'	(2 ^{195}Pt nuclei, X, X', 7.4% abundance)
AA'XX'Y	(3 ^{195}Pt nuclei, X, X', Y, 3.7% abundance)

TABLE 5. Fractional atomic coordinates of non-hydrogen atoms for $Pt_3(\mu\text{-}CNC_8H_9)_3(PCy_3)_3$ with estimated standard deviations in parentheses

Atom	x	y	z
Pt(1)	0.30840(3)	0.24398(2)	0.20598(3)
Pt(2)	0.10841(3)	0.24506(2)	0.06484(3)
Pt(3)	0.24963(3)	0.24482(2)	0.00477(3)
P(1)	0.4180(2)	0.2225(1)	0.3677(2)
P(2)	−0.0686(2)	0.2249(1)	0.0093(2)
P(3)	0.2903(2)	0.2251(1)	−0.1208(2)
C(111)	0.3394(9)	0.1790(6)	0.4214(9)
C(112)	0.238(1)	0.1245(7)	0.338(1)
C(113)	0.171(1)	0.0965(8)	0.382(1)
C(114)	0.235(1)	0.0661(8)	0.480(1)
C(115)	0.331(1)	0.1175(8)	0.562(1)
C(116)	0.402(1)	0.1479(7)	0.519(1)
C(121)	0.5101(9)	0.2997(6)	0.4656(9)
C(122)	0.602(1)	0.2964(7)	0.571(1)
C(123)	0.675(1)	0.3649(8)	0.630(1)
C(124)	0.618(1)	0.4088(8)	0.649(1)
C(125)	0.520(1)	0.4121(8)	0.545(1)
C(126)	0.447(1)	0.3436(7)	0.483(1)
C(131)	0.5121(9)	0.1717(6)	0.3835(9)
C(132)	0.459(1)	0.1055(7)	0.312(1)
C(133)	0.538(1)	0.0619(9)	0.337(1)
C(134)	0.636(1)	0.0994(9)	0.333(1)
C(135)	0.683(1)	0.1664(8)	0.397(1)
C(136)	0.602(1)	0.2076(8)	0.369(1)
C(211)	−0.1521(8)	0.1808(5)	−0.1303(8)
C(212)	−0.272(1)	0.1523(7)	−0.172(1)
C(213)	−0.332(1)	0.1226(8)	−0.287(1)
C(214)	−0.286(1)	0.0689(8)	−0.309(1)
C(215)	−0.171(1)	0.0966(8)	−0.269(1)
C(216)	−0.108(1)	0.1271(7)	−0.155(1)
C(221)	−0.1224(9)	0.1754(6)	0.0790(9)
C(222)	−0.100(1)	0.1081(8)	0.089(1)
C(223)	−0.156(1)	0.0678(9)	0.138(1)
C(224)	−0.127(1)	0.1028(9)	0.242(1)
C(225)	−0.137(1)	0.1732(7)	0.240(1)
C(226)	−0.082(1)	0.2105(7)	0.190(1)
C(231)	−0.1103(9)	0.3017(6)	0.0123(9)
C(232)	−0.095(1)	0.3468(7)	−0.060(1)
C(233)	−0.107(1)	0.4147(8)	−0.039(1)
C(234)	−0.213(1)	0.4109(8)	−0.047(1)
C(235)	−0.229(1)	0.3673(8)	0.023(1)
C(236)	−0.221(1)	0.2985(7)	−0.002(1)
C(311)	0.3982(9)	0.1819(6)	−0.0748(9)
C(312)	0.417(1)	0.1545(7)	−0.160(7)
C(313)	0.515(1)	0.1272(8)	−0.111(1)
C(314)	0.502(1)	0.0746(8)	−0.051(1)
C(315)	0.483(1)	0.1019(8)	0.033(1)
C(316)	0.388(1)	0.1296(7)	−0.012(1)
C(321)	0.1834(9)	0.1736(6)	−0.2511(9)
C(322)	0.095(1)	0.2081(7)	−0.314(1)
C(323)	0.021(1)	0.1683(8)	−0.428(1)
C(324)	−0.028(1)	0.0983(8)	−0.428(1)
C(325)	0.055(1)	0.0654(8)	−0.360(1)
C(326)	0.133(1)	0.1050(7)	−0.249(1)
C(331)	0.3399(9)	0.3024(6)	−0.1564(9)
C(332)	0.350(1)	0.3010(7)	−0.252(1)
C(333)	0.374(1)	0.3693(7)	−0.275(1)
C(334)	0.476(1)	0.4133(8)	−0.184(1)
C(335)	0.473(1)	0.4163(8)	−0.081(1)
C(336)	0.444(1)	0.3461(7)	−0.062(1)
N(4)	0.1973(7)	0.3030(5)	0.2966(7)
C(4)	0.1924(8)	0.2669(5)	0.2248(8)
C(41)	0.1476(9)	0.3483(6)	0.3132(9)
C(42)	0.117(1)	0.3392(7)	0.387(1)
C(43)	0.068(1)	0.3845(8)	0.404(1)
C(44)	0.048(1)	0.4331(9)	0.352(1)
C(45)	0.085(1)	0.4452(8)	0.282(1)
C(46)	0.134(1)	0.4006(7)	0.262(1)
C(421)	0.140(1)	0.2844(7)	0.450(1)
C(461)	0.175(1)	0.4146(7)	0.188(1)
N(5)	0.0608(7)	0.3034(4)	−0.1286(7)
C(5)	0.1065(9)	0.2691(6)	−0.0668(8)
C(51)	0.0768(9)	0.3485(6)	−0.1885(9)
C(52)	0.165(1)	0.4031(7)	−0.143(1)
C(53)	0.179(1)	0.4473(8)	−0.205(1)
C(54)	0.099(2)	0.435(1)	−0.310(2)
C(55)	0.012(1)	0.3854(9)	−0.353(1)
C(56)	−0.002(1)	0.3409(7)	−0.293(1)
C(521)	0.247(1)	0.4145(7)	−0.027(1)
C(561)	−0.103(1)	0.2878(8)	−0.341(1)
N(6)	0.4835(7)	0.3025(5)	0.1587(7)
C(6)	0.4012(9)	0.2698(6)	0.1394(9)
C(61)	0.5762(9)	0.3493(6)	0.2424(9)
C(62)	0.567(1)	0.4017(6)	0.294(1)
C(63)	0.660(1)	0.4456(8)	0.375(1)
C(64)	0.757(1)	0.4354(9)	0.401(1)
C(65)	0.768(1)	0.3877(8)	0.350(1)
C(66)	0.675(1)	0.3411(7)	0.267(1)
C(621)	0.461(1)	0.4138(7)	0.263(1)
C(661)	0.685(1)	0.2887(8)	0.205(1)

The $^{31}P\{^1H\}$ NMR spectrum and computer simulation are shown in Fig. 6.

2.4. *Substitution reactions of* $[Pt_3(CNC_8H_9)_{3+x}(PCy_3)_{3-x}]$ $(x = 0, 1, 2, 3)$

This and earlier work [9,10] has demonstrated that the complete series of cluster compounds of the type $[Pt_3(CNC_8H_9)_{3+x}(PCy_3)_{3-x}]$ (where $x = 0, 1, 2, 3$) may be synthesised. The substitution reactions of these clusters with CNC_8H_9, PCy_3 and CO were studied to see whether these clusters were interconvertible. These reactions are summarised in Fig. 7. The reactions of CNC_8H_9 with compounds **5** and **6** have been reported previously [9].

Reaction of one equivalent of CNC_8H_9 with $[Pt_3(\mu\text{-}CNC_8H_9)_3(PCy_3)_3]$ (**1**) involved in substitution of PCy_3 to give $[Pt_3(\mu\text{-}CNC_8H_9)_3(CNC_8H_9)(PCy_3)_2]$ (**2**). Further addition of CNC_8H_9 to **2** gave $[Pt_3(\mu\text{-}CNC_8H_9)_3(CNC_8H_9)_2(PCy_3)]$ (**3**). Compound **3** was also formed from the reaction of PCy_3 with $[Pt_3(\mu\text{-}CNC_8H_9)_3(CNC_8H_9)_3]$ (**4**). The cluster compounds **1** and **2** both reacted with CO to form $[Pt_3(\mu\text{-}CNC_8H_9)_2(\mu\text{-}CO)(CNC_8H_9)(PCy_3)_2]$ (**6**).

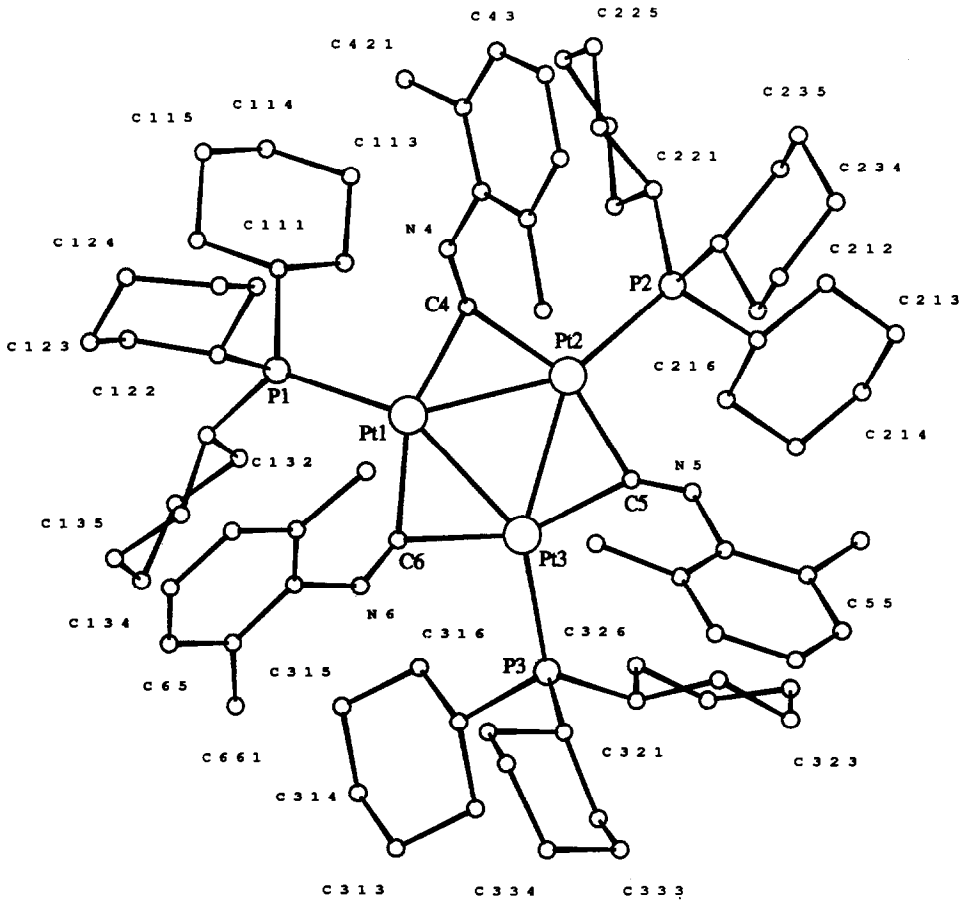

Fig. 3. Molecular structure of $[Pt_3(\mu\text{-}CNC_8H_9)_3(PCy_3)_3]$ with the hydrogen atoms omitted for clarity.

From Fig. 7 it can be seen that compounds **1** and **2** readily undergo substitution reactions with CNC_8H_9 and CO to form less crowded cluster compounds. Compounds **2** and **3** however did not undergo substitution reactions with PCy_3 to form **1** and **2**, respectively, reinforcing the previous observation [9] that it is sterically unfavourable to locate a bridging isocyanide across a $Pt_2(PCy_3)_2$ moiety. As a result, clusters containing bridging isocyanide ligands, as in compounds **1** and **2** cannot be synthesised from substitution reactions of less crowded platinum cluster compounds.

All the reactions shown in Fig. 7 occurred quantitatively, implying, although not proving, that the triangular geometry was retained throughout the reactions. The reaction scheme shown in Fig. 7 suggests that **3** and **6** are the most stable clusters in this series, since many of the synthetic reactions lead to them and none lead away from them. They presumably represent the most effective compromise of the steric and electronic effects within this series of *triangulo* cluster compounds. In general it appears that replacement of carbonyl by isocyanide is favourable electronically but limited by the additional steric constraints imposed by the bending requirements of the isocyanide ligand and compounds **3** and **6** are able to accommodate because of the reduction in the number of phosphine ligands.

TABLE 6. Pt–Pt bond lengths for selected clusters

Cluster	Pt–Pt distances	Reference
$[Pt_3(\mu\text{-}SO_2)_3(PCy_3)_3]$	2.814(1), 2.815(1), 2.813(1)	15
$[Pt_3(\mu\text{-}CO)_3(PCy_3)_3]$	2.656(2), 2.656(2), 2.655(2)	16
$[Pt_3(\mu\text{-}CO)(\mu\text{-}CNC_8H_9)_2(CNC_8H_9)(PCy_3)_2]$	2.648(1), 2.625(1), 2.627(1)	9
$[Pt_3(\mu\text{-}CNC_8H_9)_3(CNC_8H_9)_2(PCy_3)]$	2.618(1), 2.626(1), 2.654(1)	9

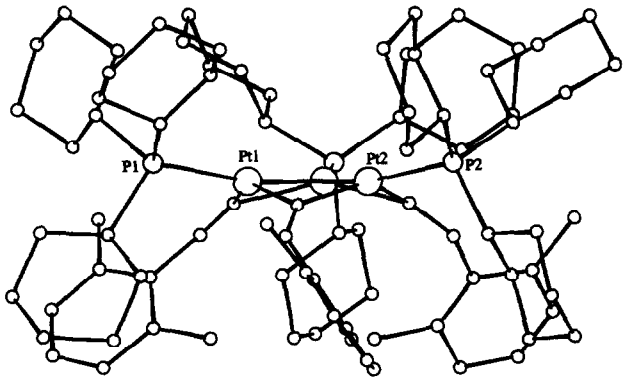

Fig. 4. Molecular structure of $[Pt_3(\mu\text{-}CNC_8H_9)_3(PCy_3)_3]$ with the hydrogen atoms omitted for clarity.

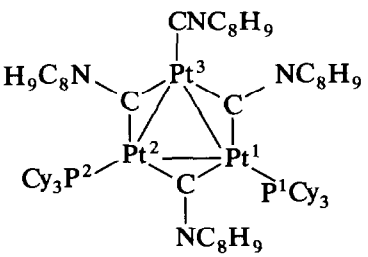

Fig. 5. Structure of $[Pt_3(\mu\text{-}CNC_8H_9)_3(CNC_8H_9)(PCy_3)_2]$.

3. Experimental details

3.1. General

Reactions were routinely carried out using standard Schlenk-line techniques under pure dry nitrogen, with dry, dioxygen free solvents. Microanalyses (C, H, N) were carried out by Mr. M. Gascoyne and his staff at this laboratory. Infra-red spectra were recorded on a Perkin-Elmer FT-1710 spectrometer as Nujol mulls between KBr discs. The $^{31}P\{^1H\}$ NMR spectra were recorded on a Bruker AM-300 spectrometer operating at 121.49 MHz and referenced to $PO(OMe)_3$ in D_2O. The NMR computer simulations were carried out by use of the Oxford University VAX computer system with a program developed by Prof. R.K. Harris, then of the University of East Anglia, and adapted for use by the late Dr. A.E. Derome in Oxford.

The compounds $Pt(COD)_2$ [19] and $[Pt_3(CNC_8H_9)_6]$ [10] were synthesised by published methods.

TABLE 7. $^{31}P\{^1H\}$ NMR data for $[Pt_3(\mu\text{-}CNC_8H_9)_3(CNC_8H_9)(PCy_3)_2]$

J (Hz)	Pt^1	Pt^2	Pt^3	P^2
P^1	4271	436	417	54
P^2	436	4271	417	

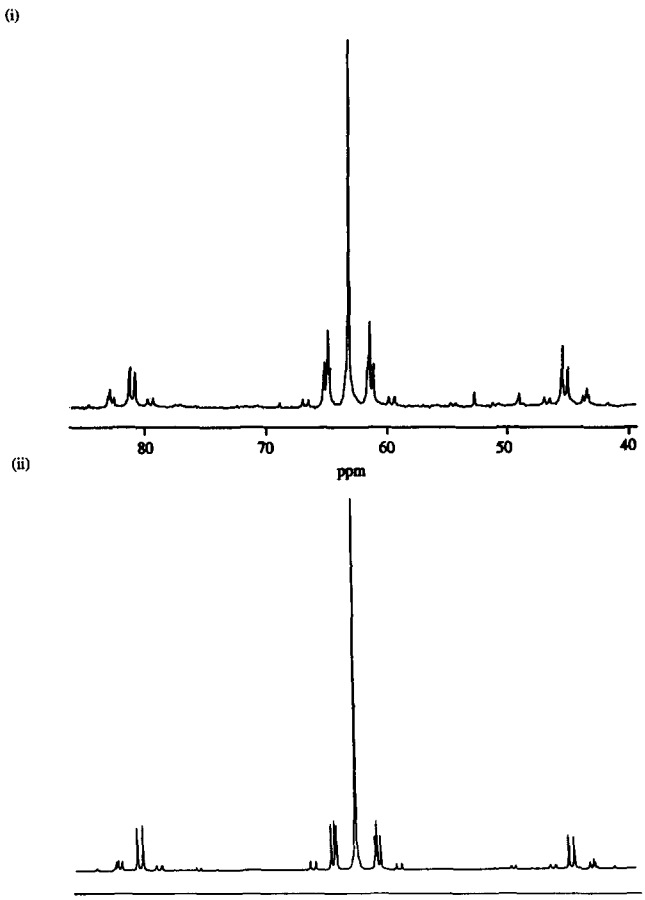

Fig. 6. $^{31}P\{^1H\}$ NMR spectrum of $[Pt_3(\mu\text{-}CNC_8H_9)_3(CNC_8H_9)(PCy_3)_2]$: (i) observed; (ii) simulated.

3.2. Synthesis

3.2.1. Synthesis of $[Pt_3(\mu\text{-}CNC_8H_9)_3(PCy_3)_3]$ (1)

A solution of PCy_3 (0.068 g, 0.24 mmol) in benzene (10 cm^3) was slowly added to one of $Pt(COD)_2$ (0.100 g, 0.24 mmol) in benzene (15 cm^3). The mixture was stirred for 10 min and CNC_8H_9 (0.032 g, 0.24 mmol) in benzene (10 cm^3) was then added, to give a red solution. After 1 h stirring the solvent was removed under reduced pressure to leave a red oil. Recrystallisation from CH_2Cl_2/MeOH gave red crystals of $[Pt_3(\mu\text{-}CNC_8H_9)_3(PCy_3)_3]$ (1). Yield 0.04 g (27%). (Found: C, 51.0; H, 6.5; N, 2.2. $C_{81}H_{126}N_3P_3Pt_3.1.5CH_2Cl_2$ requires C, 50.9; H, 6.6; N, 2.2%).

3.2.2. Synthesis of $[Pt_3(\mu\text{-}CNC_8H_9)_3(PPh_3)_3]$

A solution of PPh_3 (0.074 g, 0.28 mmol) in toluene (10 cm^3) was added dropwise to one of $Pt(COD)_2$ (0.116 g, 0.28 mmol) in toluene (20 cm^3) at 0°C. After 10 min stirring a solution of CNC_8H_9 (0.037 g, 0.28 mmol) in toluene (10 cm^3) was added. The red solution was stirred for 30 min after which the solvent was

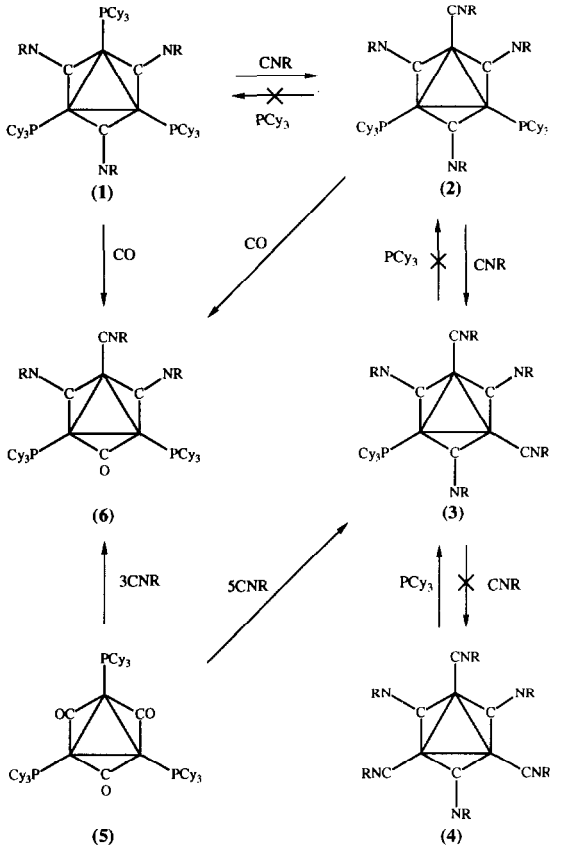

Fig. 7. Synthesis and interconversion of *triangulo*-platinum clusters ($R = C_8H_9$).

removed under reduced pressure. Recrystallisation of the residue from CH_2Cl_2/petroleum ether gave red crystals of $[Pt(\mu\text{-}CNC_8H_9)_3(PPh_3)_3]$. (Found: C, 55.5; H, 4.3; N, 2.3. $C_{81}H_{72}N_3P_3Pt_3$ requires C, 55.1; H, 4.1; N, 2.4%). ^1H NMR (CD_2Cl_2): δ 7.53–7.19 [m, 45H, C_6H_5]; 6.51–6.39 [M, 9H, C_6H_3NC]; 1.35 [S, 18H, CH_3].

3.2.3. Synthesis of $[Pt_3(\mu\text{-}CNC_8H_9)_3(PBz_3)_3]$

A solution of PBz_3 (0.074 g, 0.24 mmol) in toluene (10 cm^3) was added dropwise to one of $Pt(COD)_2$ (0.100 g, 0.24 mmol) in toluene (20 cm^3). The mixture was stirred for 10 min and a solution of CNC_8H_9 (0.032 g, 0.24 mmol) in toluene (10 cm^3) was then added. A colour change from pale yellow to red was observed. After 30 min stirring the solvent was removed under reduced pressure to leave a red oil. Recrystallisation from CH_2Cl_2/EtOH gave orange crystals of $[Pt_3(\mu\text{-}CNC_8H_9)_3(PBz_3)_3]$. Yield 0.15 g (65%) (Found: C, 57.5; H, 4.9; N, 2.2. $C_{90}H_{90}N_3P_3Pt_3$ requires C, 57.1; H, 4.8; N, 2.2%).

3.2.4. Synthesis of $[Pt_3(\mu\text{-}CNC_8H_9)_3(PMe_2Ph)_3]$

A solution of PMe_2Ph (0.041 g, 0.3 mmol) in toluene (10 cm^3) was added dropwise to one of $Pt(COD)_2$ (0.123 g, 0.3 mmol) in toluene (20 cm^3) at 0°C. After 10 min stirring CNC_8H_9 (0.039 g, 0.3 mmol) in toluene (10 cm^3) was added. The deep red solution formed was stirred for 1 h. The solvent was then removed under reduced pressure to give $[Pt_3(\mu\text{-}CNC_8H_9)_3(PMe_2Ph)_3]$ as a red oil.

3.2.5. Synthesis of $[Pt_3(\mu\text{-}CNC_8H_9)_3(PMe_3)_3]$

PMe_3 (0.023 g, 0.3 mmol) in toluene (10 cm^3) was added dropwise to one of $Pt(COD)_2$ (0.123 g, 0.3 mmol) in toluene (20 cm^3) at 0°C. After 10 min stirring CNC_8H_9 (0.039 g, 0.3 mmol) in toluene (10 cm^3) was added. The deep red solution was stirred for 1 h and the solvent removed under reduced pressure to give a red oil.

3.2.6. Synthesis of $[Pt_3(\mu\text{-}CNC_8H_9)_3(CNC_8H_9)\text{-}(PCy_3)_2]$ (2)

A solution of PCy_3 (0.068 g, 0.24 mmol) in benzene (10 cm^3) was slowly added to one of $Pt(COD)_2$ (0.150 g, 0.36 mmol) in benzene (15 cm^3). The mixture was stirred for 10 min and a solution of CNC_8H_9 (0.064 g, 0.48 mmol) in benzene (10 cm^3) was then added. The red solution was stirred for 1 h and the solvent then removed under reduced pressure to leave a red oil. Recrystallisation from CH_2Cl_2/EtOH gave orange crystals of $[Pt_3(\mu\text{-}CNC_8H_9)_3(CNC_8H_9)\text{-}(PCy_3)_2]$ (2). Yield 0.085 g (42%) (Found: C, 51.5; H, 6.1; N, 3.4. $C_{72}H_{102}N_4P_2Pt_3$ requires C, 51.8; H, 6.1; N, 3.4%.

3.2.7. Reaction of $[Pt_3(\mu\text{-}CNC_8H_9)_3(PCy_3)_3]$ (1) with CNC_8H_9

A solution of CNC_8H_9 (0.0026 g, 0.02 mmol) in toluene (10 cm^3) was added to one of $[Pt_3(\mu\text{-}CNC_8H_9)_3(PCy_3)_3]$ (1) (0.036 g, 0.02 mmol) in toluene (30 cm^3). The mixture was stirred for 30 min after which time the red solution had lightened in colour. The solvent was removed under reduced pressure and the crude product recrystallised from CH_2Cl_2/EtOH to give orange crystals of $[Pt_3(\mu\text{-}CNC_8H_9)_3(CNC_8H_9)\text{-}(PCy_3)_2]$ (2) in quantitative yield.

3.2.8. Reaction of $[Pt_3(\mu\text{-}CNC_8H_9)_3(CNC_8H_9)\text{-}(PCy_3)_2]$ (2) with CNC_8H_9

A one molar equivalent of CNC_8H_9 in toluene was added to a solution of $[Pt_3(\mu\text{-}CNC_8H_9)_3(CNC_8H_9)(PCy_3)_2]$ (2) in toluene. The mixture was stirred for 30 min and the solvent then removed under reduced pressure. The crude product was recrystallised from CH_2Cl_2/MeOH to give dark orange crystals of $[Pt_3(\mu\text{-}CNC_8H_9)_3(CNC_8H_9)_2(PCy_3)]$ (3) in quantitative yield. (Found: C, 49.4; H, 5.0; N, 4.5 $C_{63}H_{78}N_5PPt_3$ requires C, 49.7; H, 5.1; N, 4.6%). IR (Nujol): ν(CN) at 2129s, 2102vs, 1847w, 1792m, 1708vs, 1586s cm^{-1} (literature

[9] 2120s, 2090s, 1860w, 1800m, 1720s, 1587s cm^{-1}). $^{31}P\{^1H\}$ NMR (CH_2Cl_2/D_2O lock): δ 56.2 [^1J(P–Pt) 3891 Hz; ^2J(P–Pt) 449 Hz] (literature [9] δ 51.9 [^1J(P–Pt 3893 Hz; ^2J(P–Pt) 452 Hz]).

3.2.9. Reaction of $[Pt_3(\mu\text{-}CNC_8H_9)_3(CNC_8H_9)_3]$ (4) with PCy_3

A solution of PCy_3 (0.043 g, 0.15 mmol) in toluene (10 cm^3) was added to a red solution of $[Pt_3(\mu\text{-}CNC_8H_9)_3(CNC_8H_9)_3]$ (**4**) (0.209 g, 0.15 mmol) in toluene (30 cm^3). After 15 min stirring the solution had lightened in colour. The solvent was removed under reduced pressure to leave an orange solid, which was washed with petroleum ether and recrystallised from CH_2Cl_2/MeOH to give dark orange crystals of $[Pt_3(\mu\text{-}CNC_8H_9)_3(CNC_8H_9)_2(PCy_3)]$ (**3**) in quantitative yield.

3.2.10. Reaction of $[Pt_3(\mu\text{-}CNC_8H_9)_3(PCy_3)_3]$ (1) with CO

A stream of CO was bubbled through a solution of $[Pt_3(CNC_8H_9)_3(PCy_3)_3]$ (**1**) (0.03 g, 0.017 mmol) in toluene (15 cm^3) for 15 min causing an immediate lightening in colour. The solvent was removed under reduced pressure and the product recrystallised from C_6H_6/MeOH to give orange crystals of $[Pt_3(\mu\text{-}CNC_8H_9)_2(\mu\text{-}CO)(CNC_8H_9)(PCy_3)_2]$ (**6**). (Found: C, 52.7; H, 6.2; N, 2.4. $C_{64}H_{93}N_3OP_2Pt_3.2C_6H_6$ requires C, 53.0; H, 6.1; N, 2.4%). IR (Nujol): ν(CN) at 2120vs, 1724vs, 1688vs, 1586s cm^{-1} ν(CO) at 1805 cm^{-1} (literature [9] ν(CN) at 2105s, 1730s, 1695s, 1590s cm^{-1} ν(CO) at 1815s cm^{-1}). $^{31}P\{^1H\}$ NMR (CH_2Cl_2/D_2O lock): δ 68.9 [^1J(P–Pt2) 4103 Hz; ^2J(P–Pt2) 435 Hz; ^2J(P–Pt1) 437 Hz; ^3J(P–P) 55 Hz]) (literature [9] δ 64.4 [^1J(P–Pt2) 4113 Hz; ^2J(P–Pt2) 442 Hz; ^2J(P–Pt) 441; ^3J(P–P) 50 Hz]).

3.2.11. Reaction of $[Pt_3(\mu\text{-}CNC_8H_9)_3(CNC_8H_9)(PCy_3)_2]$ (2) with CO

A stream CO was bubbled through a solution of $[Pt_3(\mu\text{-}CNC_8H_9)_3(CNC_8H_9)(PCy_3)_2]$ (**2**) (0.09 g, 0.05 mmol) in toluene (20 cm^3) for 15 min causing an immediate lightening in colour. The solution was concentrated to low volume under reduced pressure and MeOH was added to give orange crystals of $[Pt_3(\mu\text{-}CNC_8H_9)_2(\mu\text{-}CO)(CNC_8H_9)(PCy_3)_2]$ (**6**).

3.3. Crystal structure determination of $[Pt_3(\mu\text{-}CNC_8H_9)_3(PCy_3)_3]$

X-ray data were collected in the Chemical Crystallography Laboratory in Oxford. The data were processed on the Chemical Crystallography VAX computer.

A single crystal of $[Pt_3(\mu\text{-}CNC_8H_9)_3(PCy_3)_3]$ with dimensions 0.40 m × 0.25 mm × 0.15 mm was mounted in a Lindemann capillary and transferred to the goniometer head of an Enraf-Nonius CAD-4 diffractometer. The experimental details associated with the crystallographic determination are summarised in Table 3. 10523 reflections were collected in two shells by $\omega/2\theta$ scans (scanwidth $0.95 + 0.35 \tan\theta$) using graphite monochromated Mo/Kα radiation, of which 9534 were unique and 6963 had $I > 3\sigma I$. An empirical absorption correction using azimuthal scan data was applied (min/max correction = 1.79, 2.38).

The positions of the three platinum atoms were deduced from a Patterson synthesis, and the remaining non-hydrogen atoms were located in subsequent Fourier difference syntheses. The hydrogen atoms were fixed in geometrically idealised positions (C–H = 1.0 Å) and were not included in the final cycles of refinement. Refinement was by full matrix least squares methods. The platinum and phosphorus atoms were assigned anisotropic thermal parameters and the carbon and nitrogen atoms isotropic thermal parameters in the final cycles of refinement. On application of a Chebychev weighting scheme the model converged at R 0.0450 and R_w 0.0533. The programs and sources of scattering factor data are given in refs. 20–22.

Acknowledgements

The SERC is thanked for financial support.

References

1 M. Green, J.A.K. Howard, M. Murray, J.L. Spencer and F.G.A. Stone, *J. Chem. Soc., Dalton Trans.*, (1977) 1509.
2 A. Moor, P.S. Pregosin and L.M. Venanzi, *Inorg. Chim. Acta, 48* (1981) 153.
3 A. Moor, P.S. Pregosin and L.M. Venanzi, *Inorg. Chim. Acta, 61* (1982) 135.
4 A. Moor, P.S. Pregosin and L.M. Venanzi, *Inorg. Chim. Acta, 85* (1984) 103.
5 J.M. Ritchey and D.C. Moody, *Inorg. Chim. Acta, 74* (1983) 271.
6 A.D. Burrows, D.M.P. Mingos and H.R. Powell, *J. Chem. Soc., Dalton Trans.*, (1992) 261.
7 S.G. Bott, O.J. Ezomo and D.M.P. Mingos, *J. Chem. Soc., Chem. Commun.*, (1988) 1048.
8 D.M.P. Mingos, I.D. Williams and M.J. Watson, *J. Chem. Soc., Dalton Trans.*, (1988) 1509.
9 C.E. Briant, D.I. Gilmour, D.M.P. Mingos and R.W.M. Wardle, *J. Chem. Soc., Dalton Trans.*, (1985) 1693.
10 A. Christofides, J.A.K. Howard, J.A. Rattue, J.L. Spencer and F.G.A. Stone, *J. Chem. Soc., Dalton Trans.*, (1980) 2095.
11 R.G. Goel, W.O. Ogini and R.C. Srivastava, *J. Organomet. Chem., 214* (1981) 405.
12 C.A. Tolman, *Chem. Rev., 77* (1977) 313.
13 Y. Koie, S. Shinoda and Y. Saito, *Inorg. Nucl. Chem. Lett., 17* (1981) 147.
14 C.E. Briant, D.G. Evans and D.M.P. Mingos, *J. Chem. Soc., Dalton Trans.*, (1986) 1535.

15 S.G. Bott, M.F. Hallam, O.J. Ezomo, D.M.P. Mingos and I.D. Williams, *J. Chem. Soc., Dalton Trans.*, (1988) 1461.
16 A. Albinati, *Inorg. Chim. Acta, 22* (1977) L31.
17 R.A. Burrow, D.H. Farrar and J.J. Irwin, *Inorg. Chim. Acta, 181* (1991) 65.
18 C.M. Hill, D.M.P. Mingos, H.R. Powell and M.J. Watson, *J. Organomet. Chem., 441* (1992) 499.
19 G.E. Heberich and B. Hessner, *Z. Naturforsch., Teil B, 34* (1979) 638.
20 G.M. Sheldrick, *SHELXS 86 Program for Crystal Structure Determination*, University of Göttingen, 1986.
21 D.J. Watkin, J.R. Carruthers and R.W. Betteridge, *CRYSTALS User Manual*, Chemical Crystallography Laboratory, University of Oxford, 1985.
22 *International Tables for X-ray Crystallography*, Kynoch Press, Birmingham, 1974.